Available online at www.sciencedirect.com
SCIENCE DIRECT®
Chemical Engineering and Processing 44 (2005) 543–555
Chemical Engineering and Processing
www.elsevier.com/locate/cep

Modeling, simulation and control of a scheibel liquid–liquid contactor Part 1. Dynamic analysis and system identification

Farouq S. Mjalli[a], Nabil M. Abdel-Jabbar[b,*], John P. Fletcher[c]

[a] *Department of Chemical Engineering, University of Qatar, Doha, Qatar*
[b] *Department of Chemical Engineering, Jordan University of Science and Technology, P.O. Box 3030, Irbid 22110, Jordan*
[c] *School of Engineering and Applied Science, Chemical Engineering and Applied Chemistry, Aston University, Birmingham, B4 7ET England, UK*

Received 15 June 2003; received in revised form 7 August 2003; accepted 26 May 2004
Available online 21 September 2004

Abstract

The liquid–liquid extraction process is well-known for its complexity and often entails intensive modeling and computational efforts to simulate its dynamic behaviour. However, rigorous mathematical models are usually impractical or are of limited usefulness for control system design. Therefore, there is a need to derive simpler models for this process. Reduced-order linear models can be derived through applying system identification on the input–output simulation data. As a first step, a rigorous model for dynamic simulation of an extraction process is developed. This model employs an improved detailed stage-wise mixing stage with backmixing and it takes into account the variation in hydrodynamics, mass transfer, and physical properties throughout the length of the extraction column. It also approximates end effects by incorporating two mixing stages at both ends in addition to calculation of mass transfer within calming zones through the use of a mass transfer weight factor. The model is validated with dynamic experimental data for a nine stage Scheibel extraction column of type I. The simulation model is shown to be accurate for prediction of process behaviour under different operating conditions. Dynamic analysis of the process is conducted on the developed rigorous simulation model. Then, system identification is applied to derive linear time-invariant reduced-order models, which relate the input process variables (*agitator speed, solvent feed flowrate and concentration, feed concentration and flowrate*) to the output process variables (*raffinate concentration and extract concentration*). The identified model predictions are found to be in a good agreement with the rigorous ones.

Keywords: Scheibel; Extraction dynamics; Liquid–liquid; Backmixing; Backflow model; Stagewise; System identification

1. Introduction

Counter-current liquid–liquid extractors are very complex. The extraction process serves a wide range of applications including nuclear fuel reprocessing, separation of metals, aromatics, pharmaceutical, petrochemical industries, waste water treatment, hydrometallurgy and food processing. Their operation needs careful consideration. A need has emerged to focus on modeling and simulation of extractors for better control system design. This has also been triggered by the necessity to understand the process behaviour under start-up, shut-down and stable operation ranges of the column.

Dynamic modeling studies of these contactors have started in the late sixties. Interesting reviews of previous work done have been given by Pollock and Johnson [1], Hanson and Sharif [2], Weinstein et al. [3] and recently by Mohanty [4]. The conventional modelling methodology applied for such processes used rigorous models based on the underlying physico-chemical phenomena present in their operation [4]. Modelling studies for the stagewise contactors reported in the past described the cascade of stages as perfectly mixed with constant volume [5]. The main concern in the development of these models is to simulate the hydrodynamics and

* Corresponding author. Tel.: +962 2 7201000x22403; fax: +962 2 7095018.
E-mail address: nabilj@just.edu.jo (N.M. Abdel-Jabbar).

0255-2701/$ – see front matter © 2004 Elsevier B.V. All rights reserved.
doi:10.1016/j.cep.2004.05.016

mass transfer within the contactor. Previously reported models suffered from either many assumptions that limited their real applicability [6,7] or that they involved detailed specifications of behaviour through the use of empirical correlations, which made the applicability of these models specific for the equipment used [8,9].

A non-equilibrium drop population stage model has been used for describing the hydrodynamics of the extraction column [10]. The effects of drop breakage, transport and inter-drop coalescence has been incorporated by the use of the so-called production terms. Molar densities have been assumed constant for both phases. This method is very sensitive to initialisation. Later on, a population balance equation model has been used to study the multistage behaviour of extraction contactors [11]. The model considered drop breakage, coalescence, and exit phenomena. These models have the disadvantage of being complicated in terms of formulation and are not relevant for control studies.

The pulsed-flow model [12] has been used to predict the operating conditions and performance of the extractive separation of the rare earth metals. The main criticisms of this work are; firstly, discrete sequences of steps in the time domain have been used to approximate the dynamic model. Secondly, stage efficiency has been calculated from steady state profiles and this does not necessarily represent the true transient approach to equilibrium in the stage. Finally, the use of constant flowrates and constant hold-ups restrict the applicability of this work.

A simpler hydrodynamic model based on Sauter mean diameter has been proposed to predict model parameters and flooding conditions [13]. The model parameters correlations used in that study were based on previous experimental studies. The solved model, however, has not been validated with experimental data and hence applicability still needs to be investigated.

Typically, the extraction models comprise a highly nonlinear large number of differential and algebraic equations (DAE) and are very complex to solve. Consequently, they have limited use for control system analysis and design studies. One approach to deal with this difficulty is to use linearization around some reference steady state condition and employ linear control theory for the design of a conventional control system. This approach is hindered by the high nonlinearity of the process which tends to limit the functionality of the designed controllers to the conditions under consideration only and any shift from these conditions causes the controllers to crash [14].

Efficient process models, however, can be derived confidently from plant testing data by using system identification techniques [15]. This is achieved by generating step changes in the input variables and collecting the output variables response data. Input–output data are then used to obtain simple reduced-order models that can describe process dynamics satisfactorily. These models may be either continuous or discrete and can have different forms such as transfer function, state-space, step response and finite impulse response models. All these types are characterised by their simplicity and relevance for real time implementation of model-based control schemes.

Motivated by the above considerations, a great need exists for adopting a modelling strategy that is capable of explaining the highly complex behaviour of the column efficiently over the whole range of operation under varying conditions of hydrodynamic and mass transfer conditions. These modelling difficulties can be tackled by using a rigorous dynamic model with variable parameters. The model parameters should be estimated as a function of operational parameters so that their values vary during simulation. This can be attained by correlating these parameters to the operating variables through a wide range of column operation. Model parameter estimation can be performed using non-linear optimisation techniques to minimise the difference between the model predictions and the experimental data. The target here is to derive a model that can be employed for transient operations and be adequate for further control system design and analysis studies.

To address these challenges, we investigate modelling and system identification of a Scheibel extraction column. This column is chosen because of its simple design and its high efficiency for laboratory as well as pilot plant scales [16]. The rigorous model developed in this study is based on the non-equilibrium mixing cell model. Backmixing is accounted for by including axial mixing terms, which are expressed as constants representing the fractions of each phase that are entrained by other phase into the adjacent stage [17]. Hydrodynamic calculations are based on a correlated fractional hold-up to enable the prediction of its transient behaviour. The drops state, namely; *stagnant*, *circulating* or *oscillating* is incorporated in the calculation of the mass transfer coefficient. Also, in order to account for the mass transfer in the calming zones, a weight factor is used in the estimation. The model parameters equations (backmixing coefficients, and mass transfer weight factor) are estimated by correlating these parameters to the operating variables through a wide range of column operation conditions. Furthermore, physical properties calculations are performed throughout the column and at each time step. All model parameters are obtained by reconciling the model predictions with the measured experimental data. Dynamic analysis is carried out to understand the process transient behaviour under different conditions. Step testing is applied on the rigorous simulation model to generate input–output response data, which are then used for multivariable system identification in order to derive simple reduced-order linear models that can adequately capture the process dynamics.

1.1. Experimental apparatus

A schematic diagram of the experimental apparatus is shown in Fig. 1. It is basically a Scheibel extraction column of type I. In this type, the column is divided into a series of wire mesh (S.S.-Polypropylene) packed calming sections followed by mixing sections. The column is made of a QVF

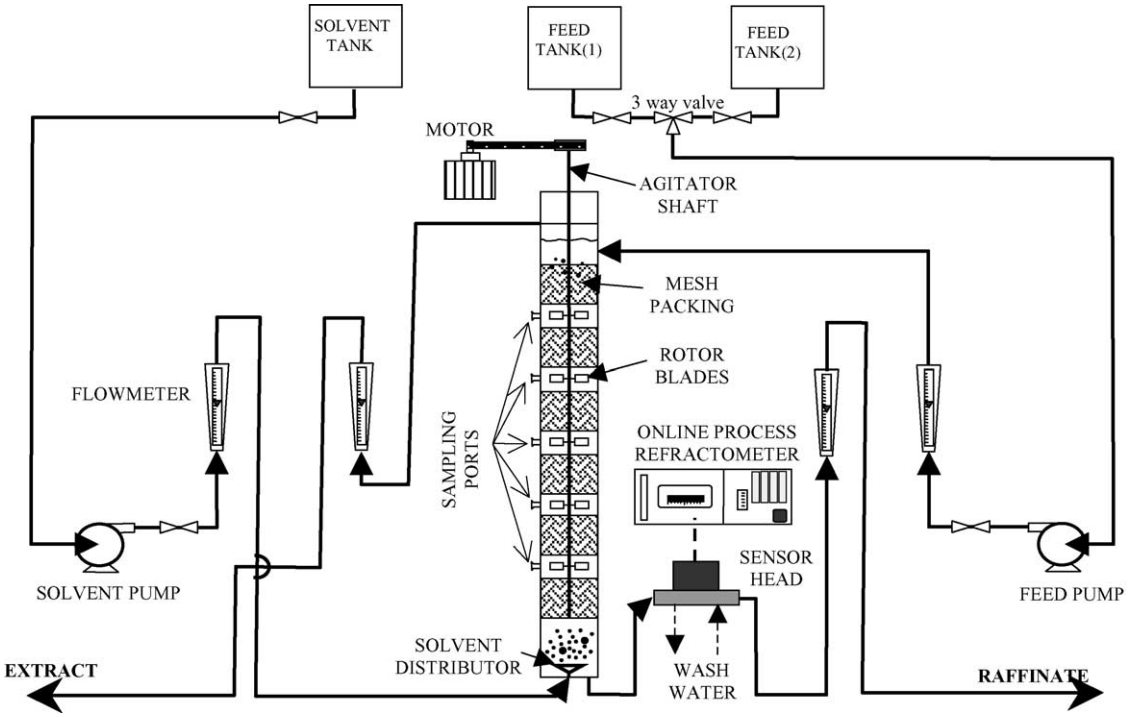

Fig. 1. Schematic diagram of the experimental apparatus.

borosilicate pipe of 8.7 cm diameter, and 185 cm length. It is divided into nine compartments each of 14.5 cm height with Dual Coalescer wire gauze packings of 12 cm height inserted in each compartment making a stage of a mixing zone and coalescence zone. The mixing zone of each stage is supplied with a hole of 15 mm in diameter on the column's wall to support the single phase sampling head probe and needle.

A test system of water–acetone–toluene was chosen for the experimental study. The feed streams are introduced countercurrently. The aqueous inlet stream is introduced at the top of the column 1.5 cm above the ninth stage whereas the solvent inlet stream is introduced at the bottom of the column through a stainless steel distributor of 4.5 cm diameter and 50 holes of 2 mm i.d. The process streams pipes are made of either stainless steel or glass pipes of 1.25 cm diameter so as to prevent any kind of corrosion or material deterioration due to the presence of solvents. The feed tanks are made of stainless steel (2 mm thick) for the same reason. They are installed on a wall-mounted support 2.5 m above ground to give enough head for the feed pumps. The raffinate concentration is monitored using an on-line refractometer (Anacon Model 47) and a PC data logging system.

1.2. Process dynamic simulation model

A dynamic version of the backflow stagewise model has been modified to handle end effects and mass transfer within calming zones. The current model has the following main features and assumptions:

(1) Flow non-idealities are handled by incorporating backflow streams opposite to the direction of the main flow streams. The values of these streams are expressed as fractions of the main flow streams.
(2) Mass transfer coefficient is calculated for each stage as function of physical properties, operational parameters and stage design specifications. Oscillating drop behaviour is assumed to model the dispersed phase due to the high degree of turbulence in the mixing zones. This assumption is adopted after careful monitoring of the dispersed phase drop behaviour using a photographic technique. The Rose–Kintner correlation [18] is used for the dispersed phase mass transfer coefficient while the Garner and Tayeban [19] correlation is used for the continuous phase.
(3) To account for the mass transfer occurring in the settling zones, a weighting factor f is introduced in the calculation of mass transfer rate term to approximate the ratio of mass transfer as $Qx_a = f \times Qx_m$ where a and m represent settling and mixing zones, respectively. These weighting factors are calculated at each stage by reconciling model predictions with the experimental data using non-linear optimisation techniques. Introducing the mass transfer weight factor will take care of any unrealistic assumption regarding the drop state behaviour. It will correct the calculated value of mass transfer at each stage.
(4) Equilibrium between phases at each stage is expressed as a distribution coefficient $m_i = y_i^*/x_i^*$. Its value is calcu-

lated for each stage from experimental data as a function of solute concentration in the raffinate phase.

(5) Hydrodynamics within stages is expressed as a fractional volume hold-up ε_i and calculated for each stage. The hold-up is measured experimentally and then correlated as a function of rotor speed and phase flow ratio. These correlations are used to predict the initial column hold-up profile in the model simulation.

(6) The physical properties of the two phases are considered as variables throughout the column and are calculated for each stage as functions of concentration, column geometry, and operational parameters.

(7) In order to approximate the damping and delaying action of the phase separation volumes (single phase) located between the interfaces and the contactor ends, a form of delay must be added to the theoretical model. This is attained by considering the volume between the interface and the sampling tube as comprising a perfectly mixed, single-phase stage without mass transfer.

A schematic drawing of the modelled contactor with the flow arrangement is shown in Fig. 2. The aqueous and organic mixing stages are modelled without the mass transfer rate term which is present in other stages. The details of the inside streams for the contactor are shown in Fig. 2. As shown in the figure, the stages have been numbered starting at the bottom of the contactor towards the top, with stages number *0* and *N* + 1 denoting the bottom and top mixing stages (without mass transfer), respectively.

Under the above assumptions, the model equations to predict flowrates and concentrations of both phases encompass the following sets of equations:

1.3. Hydrodynamic equations

The hold-up at each stage depends on the fractional hold-up coefficient ε_i. For any stage i: 1...N, it can be expressed as:

$$h_{x_i} = V(1-\varepsilon_i), \quad h_{y_i} = V\varepsilon_i \tag{1.a}$$

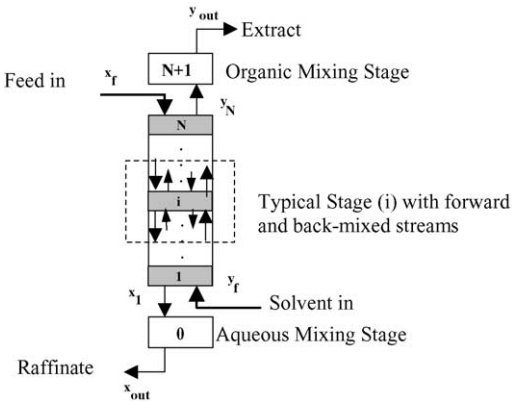

Fig. 2. Schematic diagram of the modified mixing stage model with back-mixing.

For the mixing stages (stages 0 and $N+1$) these equations represent boundary conditions and are expressed as:

$$h_{x_0} = V, \quad h_{y_0} = 0 \tag{1.b}$$

$$h_{x_{N+1}} = 0, \quad h_{y_{N+1}} = V \tag{1.c}$$

1.4. Solute free material balance

The Solvent and the Feed can be assumed to be practically immiscible, hence a solute-free material balance can be performed over each stage to calculate the flowrates at each stage. After rearranging variables, the flowrates of the two phases at any stage i: 2, ..., $N-1$ are expressed as:

$$S_i = \frac{\beta S_{i+1}(1-y_{i+1}) + (1+\beta)S_i(1-y_i) + h_{y_i}(\mathrm{d}y_i/\mathrm{d}t)}{[(1+\beta)(1-y_i)]} \tag{2.a}$$

$$R_i = \frac{[(1+\alpha)R_{i+1}(1-x_{i+1}) + \alpha R_{i-1}(1-x_{i-1}) + h_{x_i}(\mathrm{d}x_i/\mathrm{d}t)]}{[(1+\alpha)(1-x_i)]} \tag{2.b}$$

for stages 1 and N the equations will be:

$$S_1 = \left[\frac{\beta S_2(1-y_2) + S_\mathrm{f}(1-y_\mathrm{f}) + h_{y_1}(\mathrm{d}y_1/\mathrm{d}t)}{[(1+\beta)(1-y_1)]}\right] \tag{2.c}$$

$$R_1 = \left[\frac{(1+\alpha)(1-x_2)R_2 + h_{x_1}(\mathrm{d}x_1/\mathrm{d}t)}{[(1+\alpha)(1-x_1)]}\right] \tag{2.d}$$

$$S_N = \left[(1+\beta)S_{N-1}(1-y_{N-1}) + h_{y_N}\frac{\mathrm{d}y_N}{\mathrm{d}t}\right] \Big/ \left[(1+\beta)(1-y_N)\right] \tag{2.e}$$

$$R_N = \left[\frac{R_\mathrm{f}(1-x_\mathrm{f}) + \alpha R_{N-1}(1-x_{N-1}) + h_{x_N}(\mathrm{d}x_N/\mathrm{d}t)}{[(1+\alpha)(1-x_N)]}\right] \tag{2.f}$$

and for the mixing stages the feeds are the input to the stages, hence the flowrates boundary values can be expressed as:

$$S_0 = S_\mathrm{f} \tag{2.g}$$

$$R_0 = \left[\frac{R_1(1-x_1) + h_{x_0}(\mathrm{d}x_0/\mathrm{d}t)}{[(1-x_0)]}\right] \tag{2.h}$$

$$S_{N+1} = \left[\frac{S_\mathrm{out}(1-y_\mathrm{out}) + h_{y_{N+1}}(\mathrm{d}y_{N+1}/\mathrm{d}t)}{[(1-y_N)]}\right] \tag{2.i}$$

$$R_{N+1} = R_\mathrm{f} \tag{2.j}$$

1.5. Component material balance

The concentrations at each stage were calculated from a solute mass balance. The general equations are expressed as:

$$\frac{dx_i}{dt} = \frac{[(1+\alpha)R_{i+1}x_{i+1} + \alpha R_{i-1}x_{i-1} - (1+2\alpha)R_i x_i - Q_{x_i}]}{h_{x_i}} \quad (3.a)$$

$$\frac{dy_i}{dt} = \frac{[\beta S_{i+1}y_{i+1} + (1+\beta)S_{i-1}y_{i-1} - (1+2\beta)S_i y_i + Q_{x_i}]}{h_{y_i}} \quad (3.b)$$

For the stages 1 and N the equations are expressed as:

$$\frac{dx_1}{dt} = \frac{[(1+\alpha)R_2x_2 - (1+\alpha)R_1x_1 - Q_{x_1}]}{h_{x_1}} \quad (3.c)$$

$$\frac{dy_1}{dt} = \frac{[\beta S_2y_2 + S_f y_f - (1+\beta)S_1y_1 + Q_{x_1}]}{h_{y_1}} \quad (3.d)$$

$$\frac{dx_N}{dt} = \frac{[R_f x_f + \alpha R_{N-1}x_{N-1} - (1+\alpha)R_N x_N - Q_{x_N}]}{h_{x_N}} \quad (3.e)$$

$$\frac{dy_N}{dt} = \frac{[(1+\beta)S_{N+1}y_{N+1} - (1+\beta)S_N y_N + Q_{x_N}]}{h_{y_N}} \quad (3.f)$$

and the boundary mixing stages equations are:

$$\frac{dx_0}{dt} = \frac{[R_1x_1 - R_{out}x_{out}]}{h_{x_0}} \quad (3.g)$$

$$\frac{dy_0}{dt} = 0, \quad y_0 = y_f \quad (3.h)$$

$$\frac{dx_{N+1}}{dt} = 0, \quad x_{N+1} = x_f \quad (3.i)$$

$$\frac{dy_{N+1}}{dt} = \frac{[S_N y_N - S_{out}y_{out}]}{h_{y_{N+1}}} \quad (3.j)$$

1.6. Equilibrium and rate equations

No mass transfer is assumed in the mixing stages, and the single solute mass transfer rate at each stage is expressed as: $Q_{x_i} = K_{x_i}a_i V(x_i - x_i^*)$where x_i^* is the concentration of solute in the aqueous phase which would be in equilibrium with the local organic phase concentration.

Equilibrium concentrations are expressed as a function of the mass distribution coefficient at any stage as: $y_i^* = m_i x_i^*$.

Values of backmixing coefficients (α, β), mass transfer weighting factor (f) are calculated using steady state optimisation of the experimental profiles whereas values of mass transfer distribution coefficient (m), distribution coefficient (D_c, D_d) for both phases and physical properties (ρ_c, ρ_d, η_c, η_d, σ) for both phases are correlated as functions of operational parameters. The details of these model parameters are explained in the next section.

In the above equations, each combined mixing and calming zone is represented by a single stage in the model, the number of these stages N was set to nine plus two mixing stages at the two ends of the column. This set of $8(N+2) - 4$ equations is sorted starting from the bottom of the column where the light phase enters the column and proceeds towards the top of the column where the heavy phase enters.

The above model equations were solved numerically using the well-known *DDASSL* stiff DAE equation solver [20]. Simulations were carried out for both positive and negative steps in rotor speed, solvent and feed flow rates and concentrations and model outputs were recorded. The model predicted profiles were then compared to the experimental profiles using the mean relative absolute error (MRAE) for both phases. The MRAE is calculated as:

$$\text{MRAE} = \frac{1}{N}\sum_{i=1}^{N}\frac{|x_i^{exp} - x_i^{pre}|}{x_i^{pre}} \quad (4)$$

where the x_i^{exp}: the experimental concentration value at the ith stage, x_i^{pre}: the model predicted concentration value at the ith stage.

2. Rigorous model parameter estimation

The developed model includes some parameters which are estimated using empirical correlations. These parameters are chemical system and column geometry specific. They involve: fractional hold-up coefficient, Sauter mean diameter, mass transfer coefficient, distribution coefficient, mass transfer weight factor, backmixing coefficients and physical properties. The hydrodynamics in each stage is expressed in terms of fractional hold-up coefficient ε_i. The dispersed phase droplet diameter is expressed as Sauter mean diameter d_{32}. These two parameters (ε_i and d_{32}) are calculated as explained in the following sections.

The extract phase fractional hold-up coefficient at each stage is correlated as a function of rotor speed (N) and the phase flow ratio at each stage F_i. The correlation is given as:

$$\varepsilon_i = b_1 + b_2 N^{b_3} + b_4(NF_i)^{b_5} \quad (5)$$

where $F_i = S_i/R_i$: phase flow ratio at stage i and b_i: are correlation constants given in Table 1.

For calculating the mass transfer interfacial area, an estimate of the average drop diameter is needed. The correlation

Table 1
Values of correlations coefficients of the model parameters

Index	Phase flow ratio (k_i)	Continuous phase backmixing coefficient (h_i)	Hold-up coefficient (b_i)
1	0.200	−2.859	0.056
2	3.613	−2.463	5.07×10^{-9}
3	−2.257	−0.800	8.284
4	0.280	0.156	8.28×10^{-4}
5	0.553	2.000	1.774
6	−0.258	4.031	–
7	0.278	−0.100	–

given by Bonnet and Jeffreys [21] for the same ternary system is used for the prediction of drop diameter as a function of hold-up and Weber dimensionless number as:

$$d_{32i} = d_r(1.763 + 16.117\varepsilon_i)We^{-0.907} \quad (6)$$

where We_i: Weber dimensionless number $= d_r^3 N^2 \rho_{ci}/\sigma_i$, N: rotor speed (s^{-1}), d_r: rotor diameter (cm), ρ_{ci}: continuous phase density at stage (i) (g/cm^3) and σ_i: interfacial surface tension (g/cm^2).

The solute mass transfer from one phase to another depends significantly on the drop state. Using single drop models Al-Aswad et al. [22] have related the overall mass transfer coefficient to the three drop regimes namely; stagnant, circulating and oscillating drops. They calculated the overall mass transfer coefficient from the following equation:

$$K_{cal} = K_S P_S + K_C P_C + K_O P_O \quad (7)$$

where P_S, P_C and P_O are the volume fraction of drops in the stagnant, circulating and oscillating drop regimes, respectively and K_S, K_C and K_O are the overall mass transfer coefficients relating to each regime.

The overall mass transfer coefficient based on the raffinate phase is calculated by applying the two-film theory [23]. This has been done for each stage i, as a function of the two mass transfer film coefficients; k_c for the continuous phase [24] and k_d for the dispersed phase [25].

It is assumed that the interfacial area for mass transfer is equal to the total surface area of all drops, and hence the interfacial area coefficient at any stage a_i can be expressed as:

$$a_i = \frac{6\varepsilon_i V_i}{d_{32i}} \quad (8)$$

where $V_i = ((\pi D^2)/4)H_s$, D: column diameter (cm) and H_s: stage height (cm).

As mentioned in the model assumptions, a weight factor is introduced in the calculation of mass transfer rate Q_{xi} in order to account for the limitation in the assumption of drop behaviour, and also for the assumption of no mass transfer in the settling zone. To account for backmixing in the two phases, the backmixing coefficients (α, β) are considered in the modelling study.

Due to lack of experimental measurements of the mass transfer weighting factor and backmixing coefficients, there is a need to estimate these model parameters using well-established estimation techniques. Non-linear optimisation methods are employed for the parameter estimation by matching the model prediction with experimental data. The experimental concentration profiles at different operating conditions were used to fit the model under consideration with the model parameters (f_i and the backmixing coefficients α, β). The objective function is similar to that of Eq. (4).

The values of the correlations parameters estimated over wide range of operating conditions are related to a set of operational variables in order to infer these parameters using simple correlations. The Mass transfer weight factor and the continuous phase backmixing coefficient are correlated to the rotor speed and phase flow ratio in the form of:

$$f_i = k_0 + k_1 N^{k_2} + k_3 F_i^{k_4} + k_5 (NF_i)^{k_6} \quad (9)$$

$$\alpha_i = h_0 + h_1 N^{h_2} + h_3 F_i^{h_4} + h_5 (\mathrm{NF}_i)^{h_6} \quad (10)$$

where N: rotor speed (s^{-1}) and F_i: phase flow ratio at stage i, k and h are correlation constants given in Table 1.

For the dispersed phase backmixing coefficient (β), the calculated values from the optimisation are found to be very small. Therefore, it is assumed that its effect is negligible and consequently, assumed zero for all runs. This finding is in agreement with the results reported by Pratt and Stevens [26] and Heyberger et al. [27]. In these studies, it has been reported that the true backmixing in mechanically agitated columns is less common within the dispersed phase, as droplets normally move only in the forward direction relative to the continuous phase. The main cause of backmixing is the circulation of continuous phase due to agitation in mixing zones.

In this work, a simple correlation is predicted for the mass transfer distribution coefficient (m_i). In this correlation, the concentration is expressed in terms of Acetone mass fraction in the continuous phase x_i:

$$m_i = 0.869 + 0.087 x_i^{-0.483} \quad (11)$$

The range of validity of this correlation is for $x_i \in [0, 0.1]$, which is sufficient for the range of operating conditions being investigated. This correlation proved to be convenient for simulation due to its simplicity.

The physical properties are considered to be variable and calculated throughout the column at each stage continuously. Table 2 lists the physical properties (*density, diffusion coefficients, interfacial tension and viscosity*) and calculation methods for both phases that are used in the model.

2.1. Dynamic analysis open loop simulations of the model

Before conducting the system identification technique, the rigorous model is tested to gain a good picture of the process behaviour in order to set the basis for the plant testing to be used for system identification.

The rigorous extraction dynamic model is utilized here to study the dynamic behaviour of the process via step testing of each of the input variables and observing the transients of the output variables. The step for each variable is selected large enough to acquire the sought dynamics, and at the same time not to exceed the operational physical limits of the process under investigation. The same step is repeated in the negative direction in order to inspect the non-linear behaviour of the process. The profiles of each variable are compared for consistency. This technique gives a very good picture of the effect of each variable and the behaviour of the process under the presence of excitations.

Table 2
Physical properties correlations used in the rigorous model

Equation no.	Property	Equation	Reference
12	Density	$\rho_c = \rho_A x_i + \rho_W(1 - x_i)$	Misek et al. [28]
		$\rho_d = \rho_A y_i + \rho_T(1 - y_i)$	
13	Diffusion coefficients	$D_c = \frac{R}{1-\varepsilon}\left[-0.171 + 0.02\frac{d_R n(1-\varepsilon)}{V_c}\right]$	Bibaud and Treybal [29]
		$D_d = d_R^2 n\left[1.3 \times 10^{-8}\, We_R^{1.54}\left(\frac{\rho_c}{\rho_c - \rho_d}\right)^{4.18} Re_R^{0.61}\right]^{-1}$	
14	Interfacial tension	$\sigma_i = 33.480 - 95.05x_i + 275.917x_i^2$	This work
15	Viscosity	$\ln \eta_d = x_T \ln \eta_T + x_A \ln \eta_A + x_T x_A G_{TA}$	Grunberg and Nissan [30]
		$\ln \eta_c = A + \frac{B}{T} + CT + DT^2$	Weast et al. [31]

2.2. Plant step testing and system identification

The liquid–liquid extraction process involves many variables, which contribute to its operation, and this makes it a multi-input multi-output (MIMO) process. These variables can be classified as follows:

Input or manipulated variables (MVs) are chosen from those variables that have direct effect on the process performance, and practically easy to actuate. In our case, these variables are; rotor speed (N) and solvent feed flowrate (S_f). The load variables (DVs) involve variables that may experience instability or fluctuation during the operation of the column. Three variables fall in this category namely; the feed concentration (x_f), the solvent feed concentration (y_f) and the raffinate feed flowrate (R_f). The controlled variables (CVs) are selected from the process outlet streams that are usually of foremost importance such as the outlet raffinate concentration (x_{out}) and the extract outlet concentration (y_{out}). A schematic diagram representing the process variables is shown in Fig. 3.

Studying the system dynamic behaviour under different operational conditions is a prerequisite to the good selection of the control scheme. This can be achieved by making some deterministic tests in the model that properly and adequately fits the actual process. The input–output relationships are studied using the open-loop dynamic response of the process, which can be determined from the process model by stepping different inputs (manipulated and disturbance variables) and recording output (control variables) responses. Starting from steady state conditions, each input is perturbed with certain magnitude that is enough to show the effect on the system dynamics. The directions and durations of amplitudes for the steps are chosen based on response strength observability, process settling time, normal operating range and measurement noise level.

The above mentioned open-loop step testing methodology is applied on the simulation model developed in the previous section, which mimics the actual plant. The Tai-Ji ID [32] system identification software package is used to process the tests responses. This programme uses the asymptotic method (ASYM) of identification developed by Zhu and Backx [33]. This method can handle test design, model order and structure selection, parameter estimation and model validation.

The Tai Ji ID program accepts the input–output step testing data and provides a set of equivalent reduced order linear models such as discrete linear state space model, discrete linear transfer function model and continuous linear transfer function model.

After selecting the identified model, it should be validated in order to make sure that the model is acceptable and can fit the plant data with minimum deviations. One way of doing this is by using the *model grading method*. In this method, the relative size of the error bound is compared with the model over the low and middle frequencies and ranking the model from A to D depending on this comparison. Based

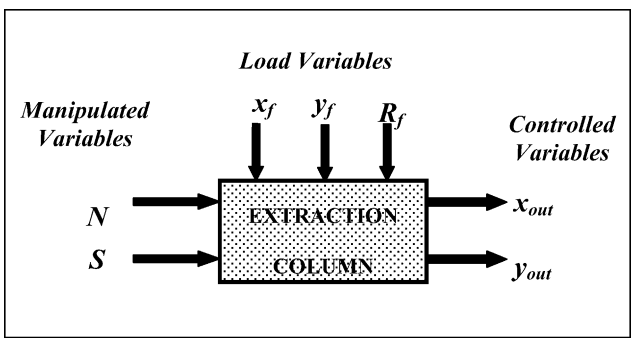

Fig. 3. Representation of variables in an extraction column as a MIMO system.

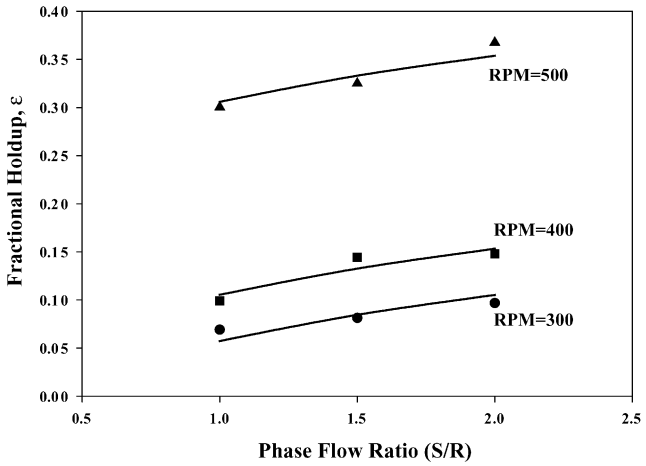

Fig. 4. The experimental fractional hold-up as a function of rotor speed and phase flow ratio.

on extensive simulations and project experience it has been shown that models with rank A or B are suitable for control system design provided that the process is not very ill-conditioned for important CVs. C grade and D grade models are not relevant for model based control system design [33].

3. Results and discussion

3.1. Model validation

The validation of dynamic response of the rigorous model is performed through conducting positive and negative step tests on the five input variables namely; *rotor speed, solvent feed flowrate, solvent feed concentration, feed flowrate and feed concentration*. For each run, the transient outlet raffinate concentration profile is calculated. A 24 min run time is shown to be enough to show the complete dynamics of the model for all tested variables.

The operating conditions used in this work are as follows:

- rotor speed = 300, 400, 500 rpm;
- solvent flowrate = 250, 375, 500 cc/min;
- raffinate flowrate = 250 cc/min;
- solvent feed concentration = 0;
- feed concentration = 0.02 wt. frac.

The two phases flowrates were selected to give phase flow ratios of 1, 1.5 and 2. For a pilot plant scale these operational data are relevant in terms of practicality and approach to flooding conditions. They provide a good basis for exploring the dynamics of the extractor. The values of fractional hold-up coefficient are given in Fig. 4.

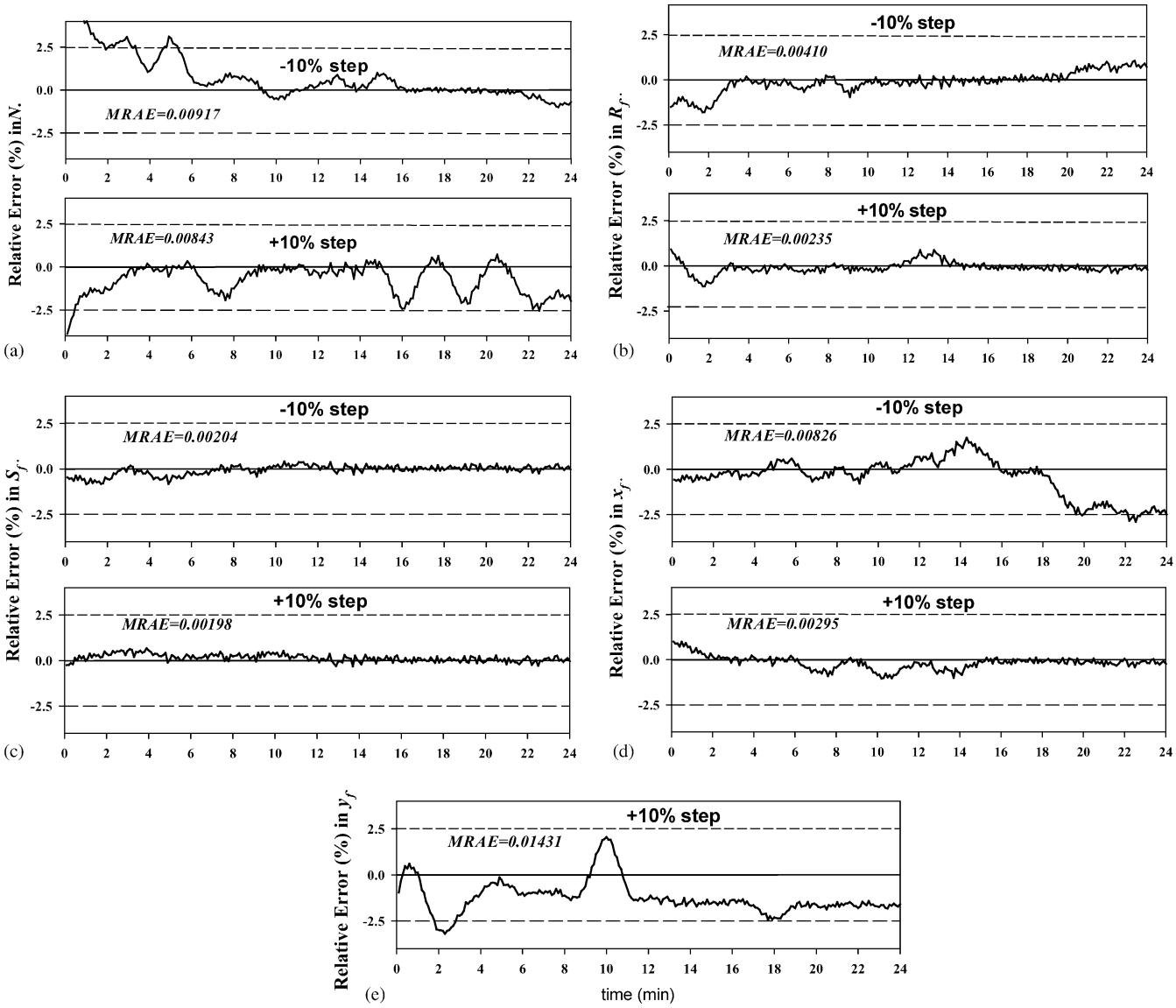

Fig. 5. Relative percentage error between experimental and predicted concentration profiles for: (a) rotor speed N; (b) feed flowrate R_f; (c) solvent flowrate S_f; (d) feed concentration x_f; (e) solvent concentration y_f.

The computer-logged raffinate phase concentration profiles are compared with the model predicted transient profiles of the model at the same conditions. In order to get an insight of how close these profiles are to each other statistically, the relative percentage error profiles for each of the previously mentioned runs are given in Fig. 5. These figures show the location of modelling error with respect to the 97.5% confidence interval indicated by the two horizontal dotted lines. The mean relative absolute error is calculated using Eq. (4) for each profile and included within the error profiles plots. Fig. 5 shows the low error values ($MRAE_x$ for the raffinate phase and $MRAE_y$ for the extract phase) which designates the good resemblance of the model to the actual column behaviour under a wide range of operating conditions.

3.2. Dynamic analysis

The effect of rotor speed and solvent feed flowrate step testing on the column outlet concentrations for both positive and negative directions is shown in Fig. 6.

Examining this figure reveals that the process reaches steady state after 10 min in the case of extract concentration profile with a time constant of less than one minute, whereas it needed 15 min for the raffinate to settle with a time constant of about 3 min. This indicates that the extract concentration has faster dynamics. Also it is clear that the shape of response is consistent for both step directions with little difference in gain. This indicates that the process is close to linearity at these conditions. The profiles of the positive and negative steps are consistent and this gives an indication of a nearly linear behaviour of the process at these operating conditions.

Fig. 7 depicts the same open loop testing results of process loads (x_f,y_f, and R_f). The same can be concluded concerning the speed of response and the linearity of the process. A relatively long dead time is noticed for response of the outlet raffinate concentration to step in feed concentration.

3.3. Model Identification

The open loop step testing is performed on the rigorous model in the form of step changes train. Each one of the five input variables (manipulated and controlled) is tested while keeping the rest constant. The signals are alternating between positive and negative square steps with lengths and amplitudes appropriate to identify process gain and dead time. The number of these steps is chosen large enough to make sure of the efficient identification of the process with acceptable accuracy. Several positive and negative square steps are applied in each test, spaning a simulation time of 350 min. The Tai-Ji ID identification program is utilized for processing the simulated input/output data. The calculated continuous transfer function model is given in Eq. (8). As can be seen from these equations the model forms are all first order functions with time delay with the exception of the (N-y_{out}) transfer function

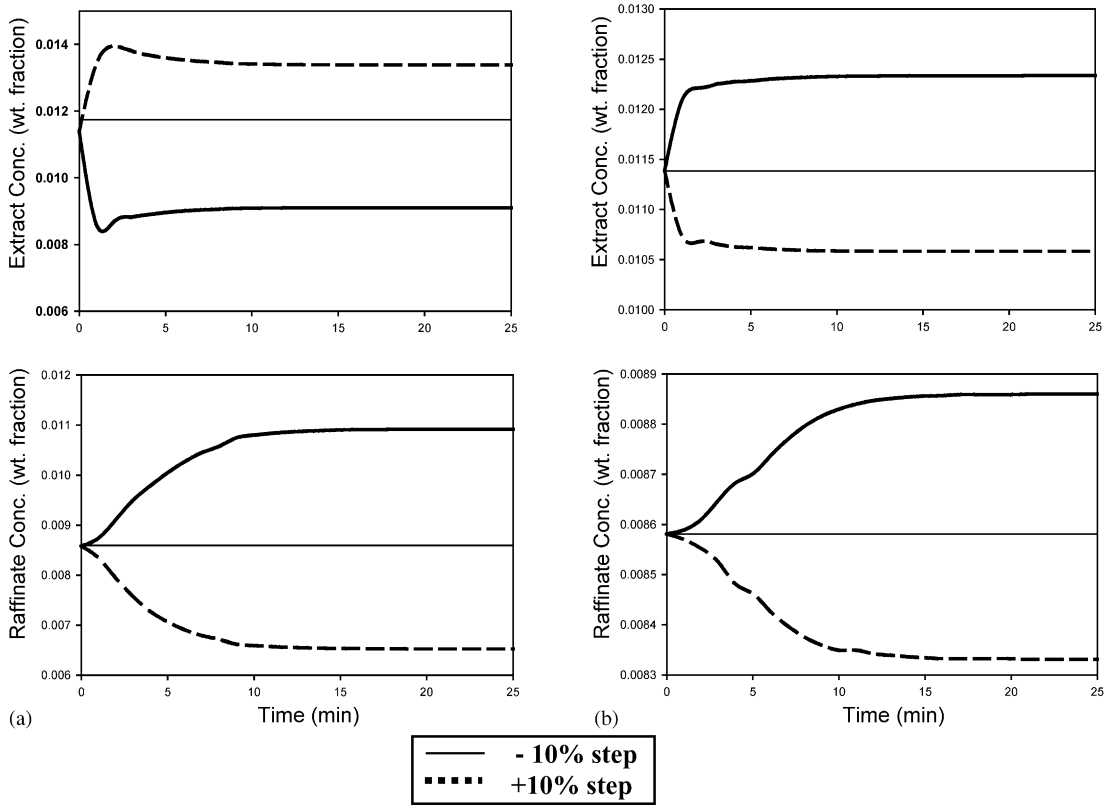

Fig. 6. Column profile for positive and negative 10% step change in process inputs: (a) rotor speed starting at a value of 400 rpm; (b) solvent concentration starting at a value of 250 cc/min.

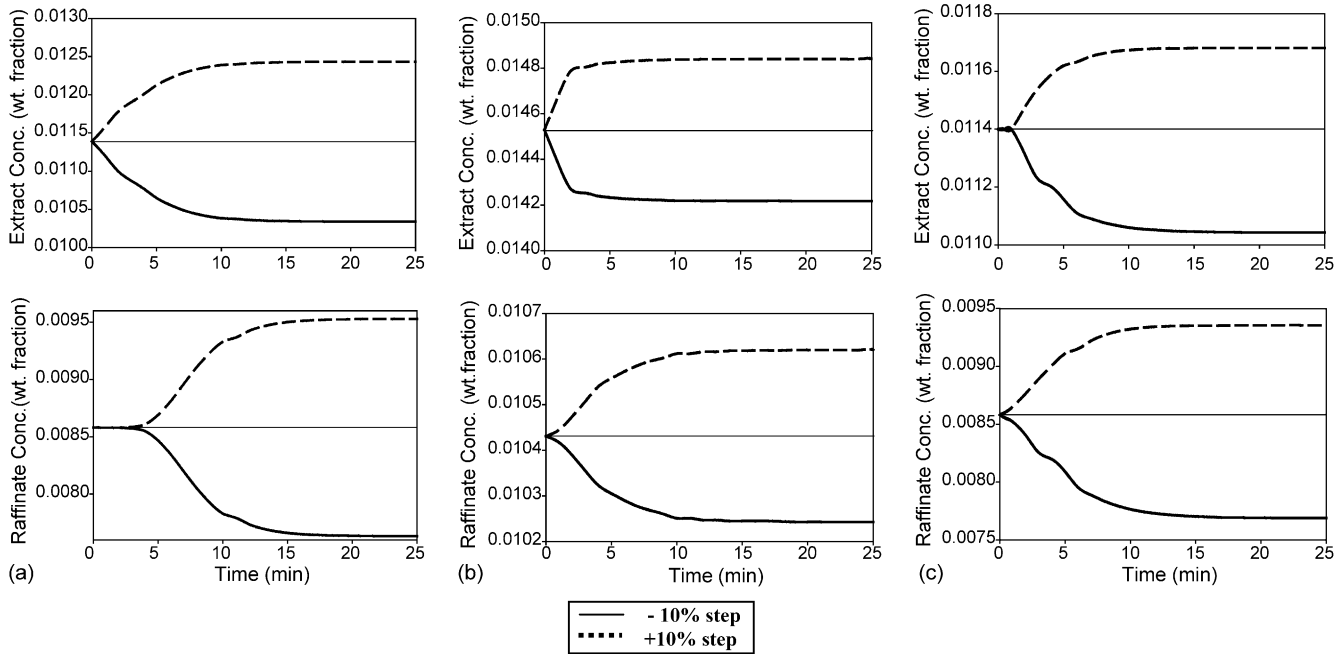

Fig. 7. Column profile for positive and negative 10% step change in process loads: (a) feed concentration starting at a value of 0.02 wt. fraction; (b) extract feed concentration starting at a value of 0.005 wt. fraction; (c) feed flowrate starting at a value of 250 cc/min.

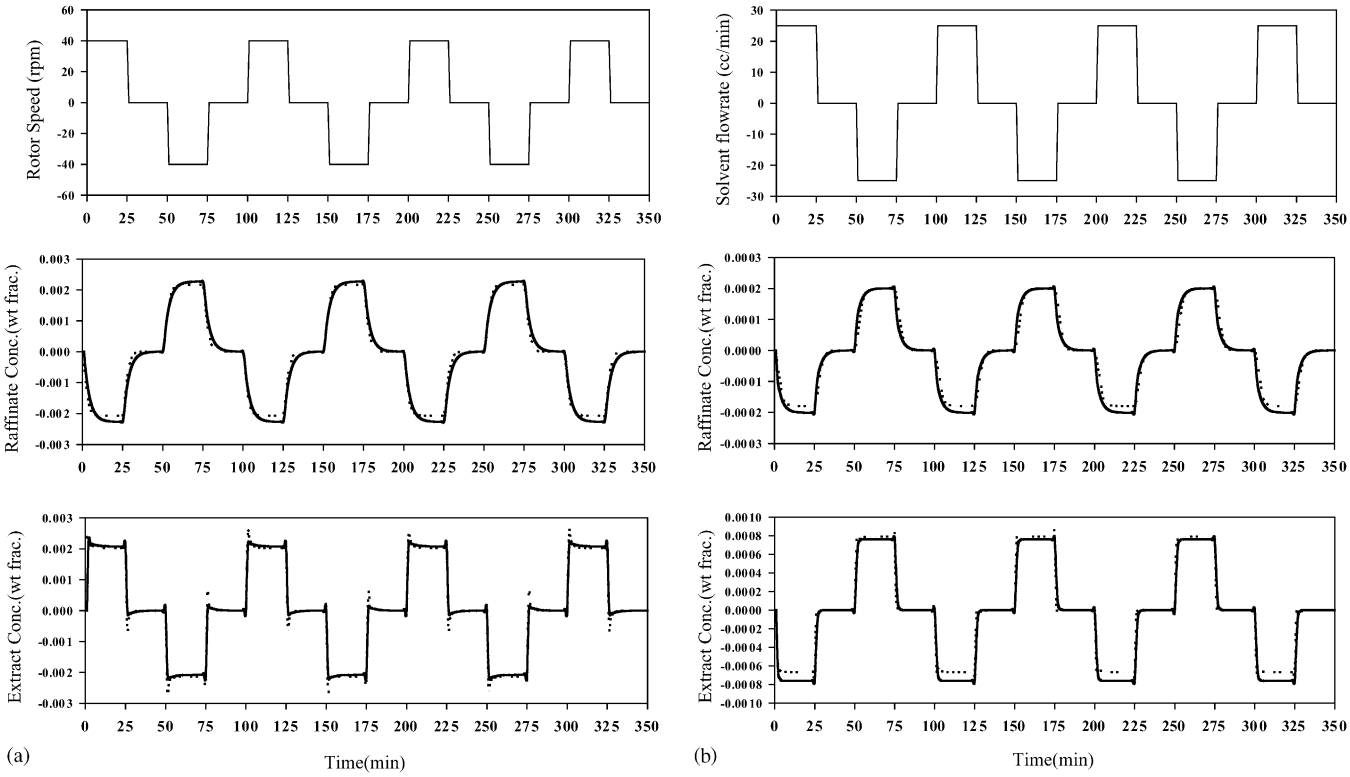

Fig. 8. Comparison of modelled to identified output profiles of process inputs due to step variations in: (a) rotor speed N; (b) solvent flowrate S_f.

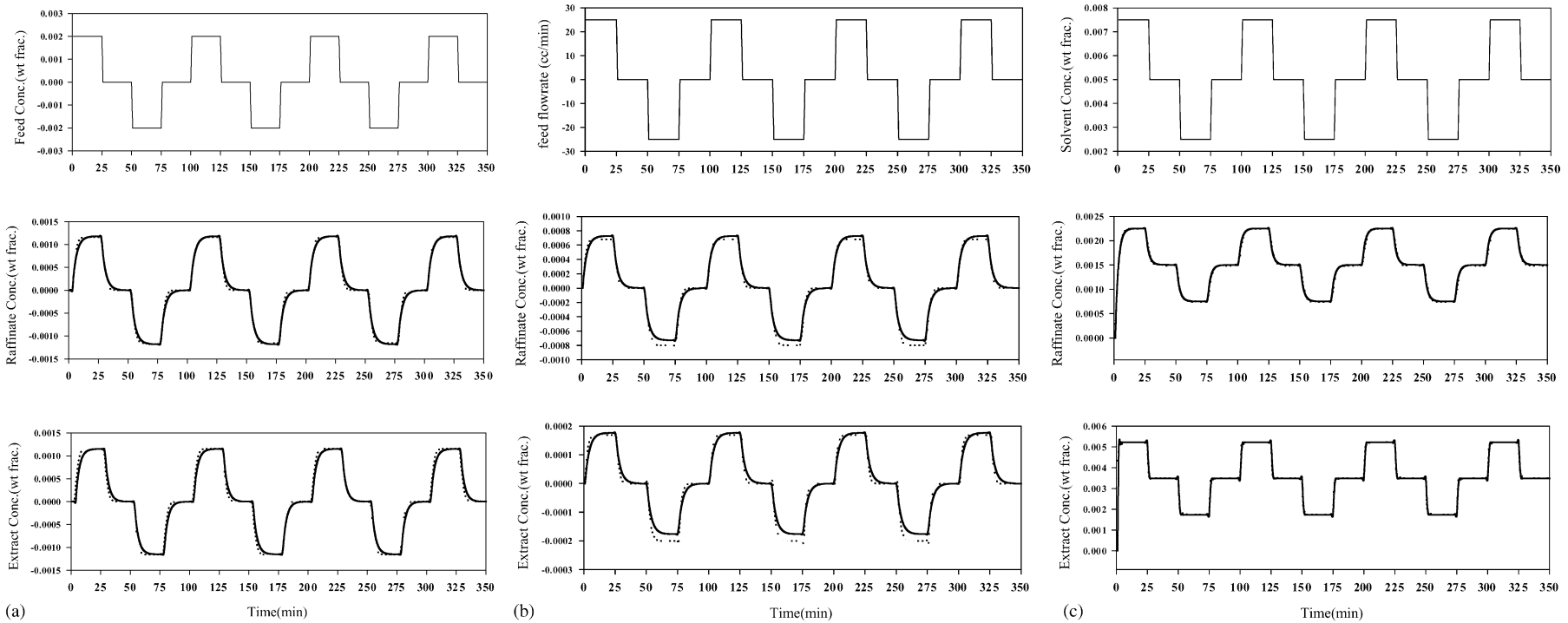

Fig. 9. Comparison of modelled to identified output profiles of process loads due to step variations in: (a) aqueous feed concentration x_f; (b) feed flowrate R_f; (c) solvent concentration y_f.

Identified profiles.
Modelled profiles.

which is a second order one.

$$\begin{bmatrix} x_{\text{out}} \\ y_{\text{out}} \end{bmatrix} = \begin{pmatrix} \dfrac{-5.45\times10^{-5}e^{-0.5s}}{3.11s+1} & \dfrac{-0.80\times10^{-5}e^{-s}}{5.03s+1} \\ \dfrac{8.2\times10^{-5}(4.28s+1)e^{-0.5s}}{(0.25s+1)(6.27s+1)} & \dfrac{-3.05\times10^{-5}e^{-s}}{0.63s+1} \end{pmatrix} \begin{bmatrix} N \\ S_{\text{f}} \end{bmatrix} + \begin{pmatrix} \dfrac{0.59e^{-4s}}{3.31s+1} & \dfrac{0.30e^{-0.5s}}{2.34s+1} & \dfrac{3.1\times10^{-5}e^{-0.5s}}{2.06s+1} \\ \dfrac{0.58e^{-0.5s}}{3.02s+1} & \dfrac{0.7e^{-0.5s}}{0.38s+1} & \dfrac{0.71\times10^{-5}e^{-s}}{3.28s+1} \end{pmatrix} \begin{bmatrix} x_{\text{f}} \\ y_{\text{f}} \\ R_{\text{f}} \end{bmatrix} \tag{12}$$

To validate this identified model of the process, both the process responses and the identified model responses are plotted in Figs. 8 and 9. Clearly, an excellent agreement between the predicted values from the rigorous model and the identified simple models are observed. The calculated modelling errors using the upper error bounds in Tai-Ji for all tested variables are found to be less than 1% and they all ranked as grade A models. This indicates that these models can be reliably applied for control system design purposes as we shall see in Part (2) of the paper.

4. Conclusions

The problem of dynamic modelling and system identification of liquid–liquid extraction columns in general and the Scheibel column in particular is considered in this work. The topic has been investigated using experimental work, rigorous modelling, dynamic analysis and reduced order system identification approach. The dynamic simulations of the Scheibel extraction column model have shown a good agreement with the measured experimental data. However, mechanistic modelling based on the underlying physics and chemistry governing the behaviour of the liquid–liquid extraction process has been found to be complex and needs a considerable computation time. Accordingly, reduced order models have been generated from the simulation input–output data via a system identification technique. The reduced order models proved to be simple and accurate enough to capture the dynamic behaviour of the process. Therefore, the development of conventional and unconventional control schemes based on these models can be practiced with confidence.

Appendix A. Nomenclature

a	interfacial area per unit height (cm^2)
A	cross sectional area of column (cm^2)
D	column diameter (cm)
f	mass transfer weight factor
F	phase flow ratio
h_x	hold-up for the aqueous phase (cm^3)
h_y	hold-up for the organic phase (cm^3)
I	identity matrix
K	overall mass transfer coefficient (cm/s)
K_x	raffinate phase mass transfer coefficient (cm/s)
m	mass transfer distribution coefficient
n	stage number n
N	rotor speed (s^{-1})
Q_x	volumetric mass transfer rate in aqueous phase (cm^3/s)
Q_y	volumetric mass transfer rate in organic phase (cm^3/s)
R	raffinate phase flowrate (cm^3/s)
R_{f}	feed flowrate (cm^3/s)
R_{out}	raffinate phase outlet flowrate (cm^3/s)
s	Laplce operator
S	extract phase flowrate (cm^3/s)
S_{f}	extract phase feed flowrate (cm^3/s)
S_{out}	extract phase outlet flowrate (cm^3/s)
t	time (s)
V	stage volume
x_{f}	feed concentration (wt. fraction)
x_n	aqueous phase concentration at stage n (wt. fraction)
x_{out}	raffinate outlet concentration (wt. fraction)
x^*	aqueous phase equilibrium concentration (wt. fraction)
y_{f}	solvent feed concentration (wt. fraction)
y_n	organic phase concentration at stage n (wt. fraction)
y_{out}	extract outlet concentration (wt. fraction)
y^*	organic phase equilibrium concentration (wt. fraction)

Greek letters

α	aqueous phase backmixing coefficient
β	organic phase backmixing coefficient
ρ	density (g/cm^3)

Subscripts

0	aqueous mixing stage
1	stage number 1
A	acetone
c	continuous phase
d	dispersed phase
f	feed
i	stage number i
N	last stage
$N + 1$	Organic mixing stage
Out	exit

Superscripts

−1	matrix inverse
T	matrix transpose
*	equilibrium

References

[1] G.C. Pollock, A.I. Johnson, The dynamic of extraction processes. Part I: Introduction and critical review of previous work, Can. J. Chem. Eng. 47 (1969) 565.

[2] C. Hanson, M. Sharif, Hydrodynamic studies on two multistage mixer-settlers, Can. J. Chem. Eng. 43 (1970) 132.

[3] O. Weinstein, R. Semiat, D.R. Lewin, Modeling, simulation and control of liquid–liquid extraction columns, Chem. Eng. Sci. 53 (2) (1998) 325–339.

[4] S. Mohanty, Modeling of liquid–liquid extraction column: a review, Rev. Chem. Eng. 16 (3) (2000) 199.

[5] R.G.E. Franks, Mathematical Modelling in Chemical Engineering, Wiley, NY, 1966.

[6] W.R. Marshall Jr., R.L. Pigford, The Application of Differential Equations to Chemical Engineering Problems, University of Delaware, 1947.

[7] R.I. Gray, The Dynamics of a Packed Gas Absorber by Frequency Response Analysis, Ph.D. Thesis, University of Tennessee, Knoxville, Tennessee, 1961.

[8] H.K., Staffin, Transient Characteristics of Continuous Extraction with Agitation, Ph.D. Thesis, Polytech. Inst. of Brooklyn, Brooklyn, NY, 1959.

[9] M. Nabeshima, M. Kitahara, C. Tanaka, M. Shuto, Dynamic simulation code DYNAC for the PUREX extraction cycle coposed of pulse columns, I. Chem. E. Symp. Ser. 103 (1987) 307–321.

[10] A. Zimmermann, C. Gourdon, X. Joulia, A. Gorak, G. Casamatta, Simulation of a multi-component extraction process by a non-equilibrium stage model incorporating a drop oopulation model, Eur. Symp. Comput. Aided Process Eng.-1 (1990) S403–S410.

[11] C. Tsouris, V.I. Kirou, L.L. Tavlarides, Drop size distribution and holdup profiles in a multistage extraction column, AIChE J. 40 (3) (1994) 407–418.

[12] J. Wichterlova, V. Rod, Dynamics behaviour of the mixer-settler cascade. Extractive separation of the rare earths, Chem. Eng. Sci. 54 (1999) 4041–4051.

[13] O. Weinstein, R. Semiat, D.R. Lewin, Modeling, simulation and control of liquid–liquid extraction columns, Chem. Eng. Sci. 53 (2) (1998) 325–339.

[14] A. Isidori, Nonlinear Control Systems, third ed., Springer-Verlag, 1995.

[15] H.W. Andersen, K.H. Rasmussen, S.B. Jørgensen, Advances in process identification, in: Proceedings of the Fourth International Conference on Chemical Process Control-CPC IV, CACHE, Padre Island, Texas, 1991, pp. 237–269.

[16] E.G. Scheibel, Scheibel Columns in Handbook of Solvent Extraction, Wily-Interscience, 1983.

[17] H.R. Foster Jr., Transient Solution to The Equations Describing a Stagewise Counter-current Extraction Process, M.Sc. Thesis, University of Washington, 1964.

[18] P.M. Rose, R.C. Kintner, Mass transfer from large oscillating drops, AIChE J. 12 (1966) 530–534.

[19] F.H. Garner, M. Tayeban, The importance of the wake in mass transfer from both continuous and dispersed phase systems, Anal. Real Soc. Espan. Fis. Quim. B56 (1960) 479–498.

[20] L.R. Petzold, A Description of DASSL: A Differential/Algebraic System Solver, SAND82-8637, September 1982.

[21] J.C. Bonnet, G.V. Jeffreys, Hydrodynamics and mass transfer characteristics of a Scheibel extractor. Part I: Drop size distribution, holdup, and flooding, AIChE J. 31 (5) (1985) 788.

[22] K.K.M. Al-Aswad, C.J. Mumford, G.V. Jeffreys, The application of drop size distribution and discrete drop mass transfer models to assess the performance of a rotating disc contactor, AIChE J. 31 (9) (1985) 1488.

[23] W.G. Whitman, The film theory of absorption, Chem. Met. Eng. 29 (1923) 147–151.

[24] F.H. Garner, M. Tayeban, The importance of the wake in mass transfer from both continuous and dispersed phase systems, Anal. Real Soc. Espan. Fis. Quim. B56 (1960) 479–498.

[25] P.M. Rose, R.C. Kintner, Mass transfer from large oscillating drops, AIChE J. 12 (1966) 530–534.

[26] H.R.C. Pratt, G.W. Stevens, Science and Practice of Liquid–Liquid Extraction, vol. 1, 1992.

[27] A. Heyberger, M. Kratky, J. Prochazka, Parameter evaluation of extractor with backmixing, Chem. Eng. Sci. 38 (8) (1983) 1303–1307.

[28] T. Misek, R. Berger, J. Schroter, Standard Test Systems for Liquid Extraction, EFCE Report GB, Rugby, 1985.

[29] R.E. Bibaud, R.E. Treybal, Axial mixing and extraction in mechanically agitated liquid extraction tower, AIChE J. 12 (1966) 472–477.

[30] L. Grunberg, A.H. Nissan, Mixture law for viscosity, Nature 164 (1949) 799–800.

[31] R.C. Weast, M.J. Astle, H.B. William, Handbook of Chemistry and Physics, 73rd ed., CRC Press Inc., Boca Raton, FL, 1993.

[32] Y.C. Zhu, Multivariable process identification for MPC: the asymptotic method and its applications, J. Proc. Cont. 8 (2) (1998) 101–115.

[33] Y.C. Zhu, T. Backx, Identification of Multivariable Industrial Processes: for Simulation, Diagnosis and Control, Springer-Verlag, London, 1993.